Materials
Views
www.MaterialsViews.com

ADVANCED
FUNCTIONAL
MATERIALS
www.afm-journal.de

FULL PAPER

Photo-Activatable Surfaces for Cell Migration Assays

Marcelo J. Salierno, Andrés J. García, and Aránzazu del Campo*

A simple material platform for advanced cell migration studies is presented. It relies on surfaces modified with photo-activatable adhesion peptides and two light exposure steps to independently trigger attachment and migration. The light-controlled exposure of adhesive ligands allows precise and selective control over integrin-mediated adhesion and migration events, including their dynamic variation. By using a microscope-coupled scanning laser, user-defined geometry, size and composition of the adhesion and migration spaces are possible and simply defined by the laser scanning parameters. Time lapse and high resolution microscopy are possible during the complete process. The miniaturization capabilities of this assay also allow (i) parallel or sequential migration experiments and controls on the same view field of the microscope, (ii) migration studies in confined and unconventional geometries or (iii) activation of migration spaces at subcellular resolution, all of these with minimum material and time consumption. The photo-activatable surfaces will allow studies of the dynamics of integrin-dependent migration processes with unprecedented flexibility, multiplexing, reproducibility, and spatiotemporal resolution.

1. Introduction

Cell migration is a critical process in embryonic morphogenesis, contributes to tissue repair and regeneration, and drives disease progression in cancer.[1–3] Migration requires the dynamic interaction between a cell and the substrate (i.e., the extracellular matrix, ECM) to which it is attached and over which it migrates in response to signaling factors, either freely diffusing (chemotaxis), tethered to the ECM (haptotaxis) or from neighbouring cells. Integrins are the major trans-membrane receptors that mediate dynamic interactions between the ECM and the intracellular actin cytoskeleton during collective migration.[4] Their extracellular domain recognizes diverse cell-binding domains in ECM proteins including fibronectin, collagen and laminin. The polarized assembly and disassembly of integrin-mediated adhesions determines the mode, speed and directionality of migration.[4] The density and spatial presentation of the adhesive ligands at the ECM,[5,6] their binding affinity and the mechanical properties of the ECM to which they are tethered (durotaxis) strongly influence this process.[7–9] Understanding how the various molecular and mechanical inputs become integrated to allow single cell or coordinated multicellular movement is challenging because of the adhesive complex structure (with over 150 different associated proteins), different sizes and morphologies (nascent adhesions, focal adhesions, focal complexes) and the transient character of integrin-mediated adhesions. Tools that allow dynamic external regulation of integrin-ECM interaction at the molecular level with precise spatial (ideally 3D) resolution and without affecting other parameters of the cellular microenvironment would significantly help for addressing and understanding relevant open questions in cell migration, i.e., the temporal and spatial dynamics of adhesions and subsequent signals during different modes of migration through 3D tissues in vivo in morphogenesis, or the switching between adhesions types and modes of migration in the context of tumor invasion and metastasis.

Several strategies that allow spatiotemporal control of the availability of adhesive ligands at the surface of a cell culture substrate have become useful platforms to mimic and control integrin-ECM interactions in the context of cell adhesion and migration.[10–15] Reported methods include (i) voltage-induced desorption of pegylated self-assembled-monolayers (SAMs) on electrodes and consequent adsorption of serum proteins,[12,13] (ii) functionalization of quinone-terminated SAMs with the cell adhesive ligand RGD upon electroactivation,[11] (iii) thermally activated exposure/occlusion of RGD ligands anchored to thermoresponsive gels, (iv) laser scanning of photocleavable pegylated layers and consequent adsorption of proteins from serum.[5,16] These methods offer limited control of the composition of the migration area and can therefore not be applied to study the dynamics of integrin-dependent migration processes. We have pioneered the use of materials functionalized with photo-activatable ("caged") RGD adhesive peptides to enable precise light-mediated control over integrin-ligand interactions.[10,14,17,18] The caged RGD peptide contains a photocleavable chromophore attached to the carboxylic side group of the aspartic acid (**Figure 1**a). This group acts as ligand for one of the two divalent cations involved in the RGD-integrin complex.[19] Introduction of the chromophore disrupts the electrostatic interactions and inhibits integrin recognition.[10,18] The cage can be removed after light irradiation at cell compatible

Dr. M. J. Salierno, Dr. A. del Campo
Max-Planck-Institut für Polymerforschung
Ackermannweg 10, 55128 Mainz, Germany
E-mail: delcampo@mpip-mainz.mpg.de
Prof. A. J. García
Woodruff School of Mechanical Engineering
and Petit Institute for Bioengineering and Bioscience
Georgia Institute of Technology
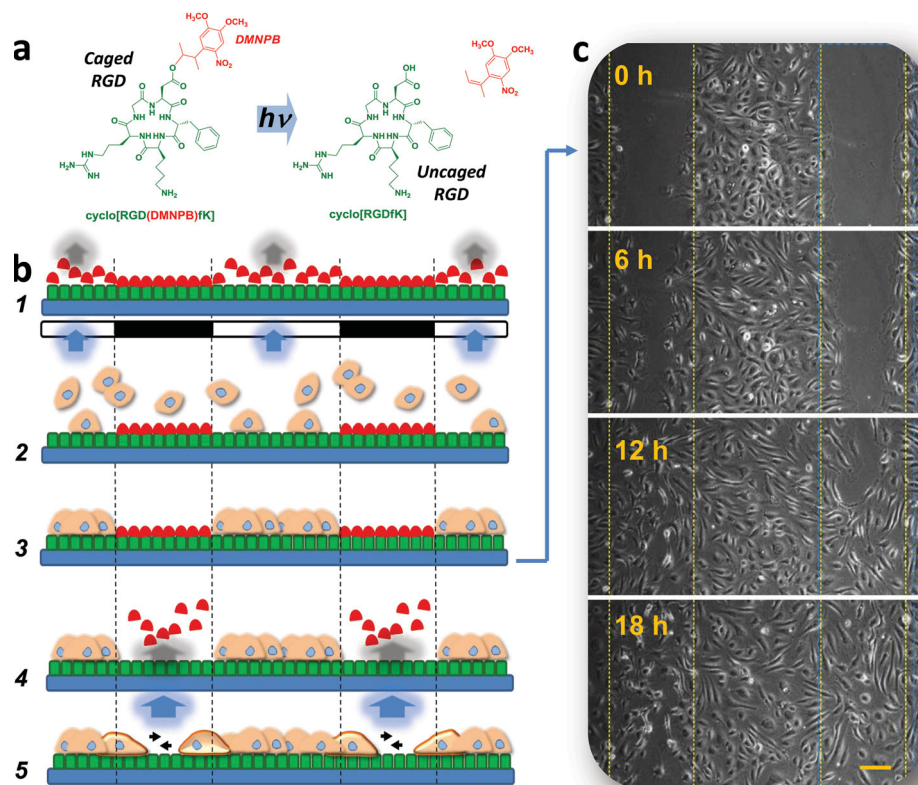Atlanta, GA 30332, USA

Figure 1. Photo-activatable cell migration assay. a) Chemical structure of the caged RGD molecule (cyclo[RGD(DMNPB)fK]) and the photolysis products (uncaged RGD and by-product). b) Steps for photo-activatable cell migration assay: 1) generation of RGD adhesive patterns after first irradiation step, 2) cell seeding, 3) monolayer formation onto the exposed areas, 4) activation of migratory paths in a second irradiation step, 5) cell migration into migratory space. c) Photo-activatable cell migration assay time lapse photographs. Migration of HUVECs on a cyclo[RGDfK] patterned SAMs is triggered after RGD activation on free spaces. Pictures lapsed every 6 h. Scale bar 200 μm.

wavelengths and doses.[18] Once photo-activated, uncaged RGD is recognized by integrins at the cell membrane and mediates the formation of integrin-mediated adhesions. As light can be focused, dosed and is readily available, in situ spatial, compositional and temporal control of active RGD sites and density is possible at any position on the surface or at any desired time point. This manuscript describes the use of the caged RGD to specifically drive and control integrin-mediated cell migration. Light exposure of commercially available substrates functionalized with caged RGD allowed us to trigger integrin-mediated migration without altering any morphological or physiological variable and using standard equipment in a biology lab. We demonstrate accurate temporal control of the migration onset, spatial definition of the migratory path location and geometry, and continuous microscopy imaging. The photo-activatable cell migration assay will enable unprecedented flexibility and precision in integrin-dependent migration studies, including single cell and collective migration assays.

It is important to note that in vitro studies of cell migration are largely focused on "wound healing assays" (WHA). In the most simple version, a confluent layer of cells is scratched with a pipette tip or a razor blade to create a cell-free region wherein border cells migrate.[20,21] Alternatives to the scratch assay include the use of a removable physical barrier to generate free space in the culture dish (i.e., Culture-insert or

CytoSelect),[22–23] confined trypsination of a cell monolayer using a microfluidic system,[20] or the application of electric fields to kill and detach cells from small electrodes deposited on the bottom of the tissue culture well.[24] Laser induced forward transfer techniques have been applied to the generation of 3D migration patterns.[25] However, none of these methods allows dynamic control over the composition of the ECM in the migration space and, in fact, most of them offer inhomogeneous and poorly defined surface compositions. In addition, mechanical stress and injury to the border cells during barrier or cell removal is present in most of the cases and this can significantly affect the results of the migration assay.[20,21,26] They only allow limited miniaturization and they do not allow continuous monitoring directly after opening the migration spaces. The photo-activatable cell migration assay (PACMA) solves these limitations and opens the door to advanced experimentation in integrin-dependent migration studies.

2. Results and Discussion

Figure 1b shows the working principle of the photo-activatable cell migration assay. Substrates functionalized with caged RGD (commercially available NEXTERION H slides or self-assembled-monolayers of COOH-terminated oligo(ethylene glycol)-thiols
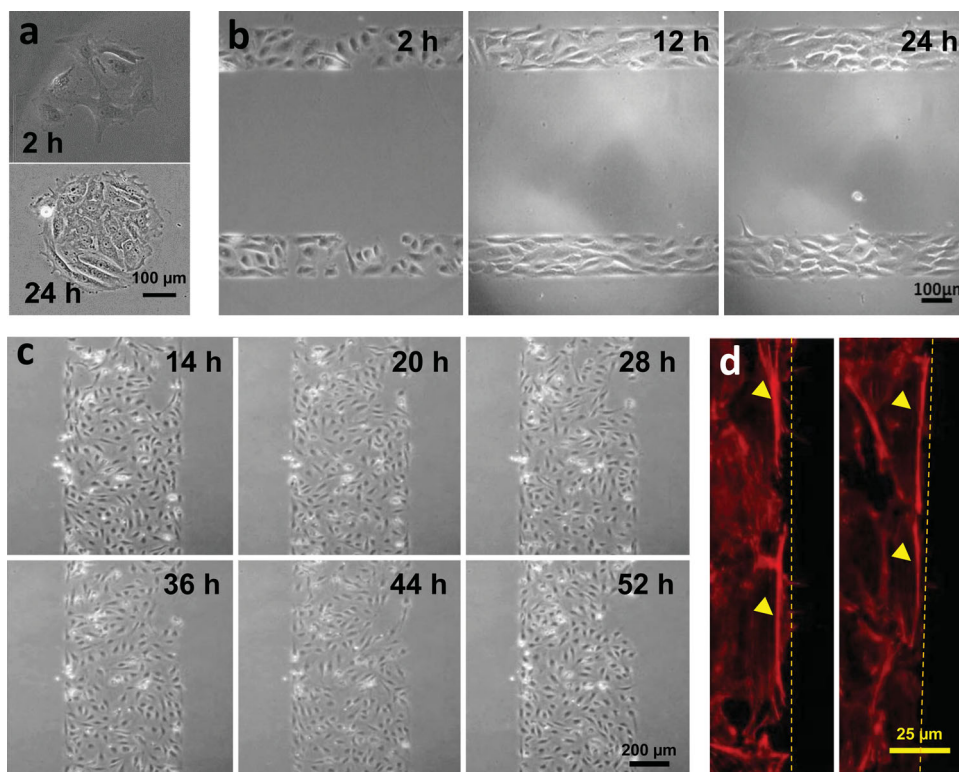
www.MaterialsViews.com

ADVANCED
FUNCTIONAL
MATERIALS
www.afm-journal.de

FULL PAPER

Figure 2. Cells on patterned monolayers with different geometrical designs remained confined to the underlying cyclo[RGDfK] pattern over several days. a) HUVEC after 2 and 24 h incubation on circular patterns of cyclo[RGDfK] modified SAMs. Scale bar corresponds to 50 μm. b) HUVEC on cyclo[RGDfK] patterned SAMs with 150 μm adhesive stripes after incubation for 2, 12, and 24 h. Scale bar 100 μm. c) HUVEC on cyclo[RGDfK] patterned NEXTERION substrates after cultivation at different times up to 52 h (Movie 1 in the Supporting Information). Scale bar 200 μm. d) High magnification fluorescence image of HUVECs at the edge of the pattern after 24 h of cell seeding. Arrow heads show actin polarization (red staining) along the edge. Dotted lines mark the edge line. Scale bar 25 μm.

on gold coated slides) were placed on a microscope equipped with a scanning laser (e.g., a confocal microscope). The substrates showed negligible cell adhesion before and after tethering of caged RGD. Site-selective light exposure (by the scanning laser using wavelengths ≤420 nm or by illumination through a patterned mask with a portable LED lamp) generated patterns of RGD (exposed) and caged RGD (unexposed) sites (Figure 1b, step 1). The size and geometry of the patterns are determined by the user (**Figure 2**a,b shows circular and stripe geometries) and easily realized by the scanning laser of the confocal microscope. After the irradiation step and incubation of the substrates with cells (e.g., HUVEC, HeLa or HT1080, Figure 1b, step 2), well-defined cell patterns were obtained (Figure 1b, step 3). Cells adhered to and occupied the photo-activated regions whereas the remaining regions that were not exposed were devoid of cells (Figure 2a,b) and therefore available for subsequent creation of migratory areas. Cells remained confined in the photo-activated patterns and the edges of the pattern remained sharply defined over more than 3 days in culture (Figure 2c, Movie 1 in the Supporting Information). A polarized actin cytoskeleton was seen on cells at the edge of the strips (Figure 2d).

Cell migration was triggered by irradiating the free space between the cell patterns in a second exposure step (Figure 1b, step 4). Irradiation uncaged the RGD adhesive motifs and made

them available for integrin recognition and subsequent cell adhesion and migration. Figure 1c and **Figure 3**a show this process with HUVECs. After irradiation, cells located within the 600 μm stripes initiated migration into the readily exposed 400 μm gap (Movie 2 in the Supporting Information). Migration proceeded with a uniform cell front over the entire length of the stripe until the complete gap was covered by cells. For comparison, a conventional scratch migration test is also shown (Figure 3b and Movie 3). For the scratch assay, migration proceeded in a haphazard and non-uniform fashion along the cell front, presumably as a consequence of the presence of cell debris in the "wound" and dead cells at the edge of the scratch that affect migration of leading cells (see marked circles in Movie 3). Figure 3c shows that approximately 30% of the cells along the edge of a conventional scratch assay were damaged after scratching. This is not the case for the photo-activatable surfaces, where all cells along the edge remained viable after illumination. Figure 3d presents the area covered by migrating cells vs. time along the same edge distance for scratch and photo-activated assays. First, the progression in the photo-activatable assay was faster (1.7-fold higher slope) than the conventional scratch assay. We attribute the faster migration rate of PACMA to higher border cell viability as well as the well-defined migratory area that lacks residual cell debris. An initial lag period was visible in PACMA, probably due to
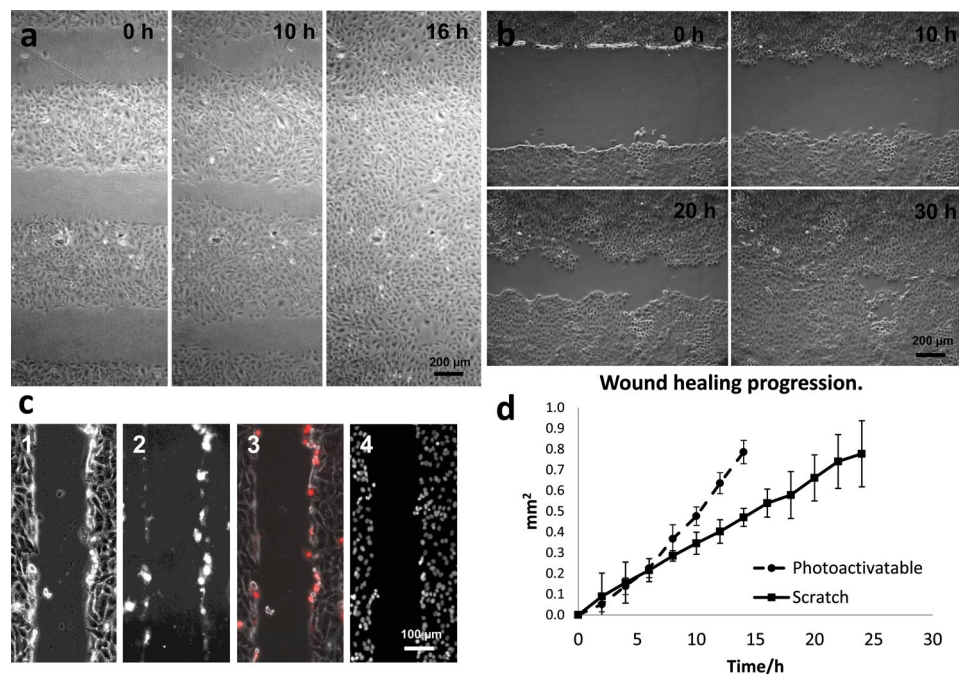
**ADVANCED
FUNCTIONAL
MATERIALS**

www.afm-journal.de

*Materials
Views*

www.MaterialsViews.com

FULL PAPER

Figure 3. Migration on photoactivatable surfaces show reduced variability and allow higher miniaturization than on scratched surfaces. a) PACMA performed with stripe monolayers of HUVECs on cyclo[RGDfK] patterned SAMs (Movie 2 in the Supporting Information). The microscope images show migrating cells at 0, 10 and 16 h after light exposure. Scale bar 200 μm. b) Scratch WHA of a HUVEC monolayer (Movie 3). Images correspond to 0, 10, 20, and 30 h after scratch. c) Pictures from the border line of a scratched cell monolayer after fixation and staining with propidium iodide and DAPI. 1) phase contrast image of the scratch, 2) epi-fluorescence image at 535 nm showing dead cells (bright), 3) photo montage with damaged cells in red, 4) stained cell nuclei (blue) for cell counting purposes. d) Wound healing progression. Data correspond to covered area by cells vs. healing time obtained from a conventional scratch test on SAMs modified with cyclo[RGDfK] or a PACMA on SAMs modified with cyclo[RGD(DMNPB)fK] (400 μm spacing between 600 μm cell stripes).

restructuring of polarized cells at the edge and initiation of migration. In addition, PACMA exhibited considerable tighter data with smaller (≈50%) standard deviation than the scratch assay. This reduced variability reflects the uniform migratory front and well-defined migratory area.

PACMA allows significant miniaturization of the cell migration patterns and, therefore, throughput enhancement and reduced variability in the experiments by providing multiple migratory lanes within a field of view. Figure 3a and Movie 2 show three 400 μm wide migration lanes imaged in parallel within the same microscopy field. For comparison, the narrowest migration lanes that could be achieved by the scratch methods were significantly wider (≈800 μm) and, therefore, only one scratch per microscopic field could be imaged using a 5× magnification objective. Attempts to generate multiple scratches within the same optical field using conventional WHA failed because the cell monolayer between scratches was lifted and partially removed from the substrate during scratching. In contrast, for the photo-activatable assay, simultaneous viewing of multiple migration fields also allowed us to evaluate different experimental and control conditions within the same field of view, either in a parallel or in a sequential manner defined by time point of the second light-activation step. Movie 4 shows a migration experiment on a scanned 400 × 800 μm space while the rest of the substrate (not exposed) provides the negative control. This allows significant savings in time and reagents and minimizes experimental error and variability in

the experiments. Fluorescence microscopy of cells expressing eGFP-vinculin demonstrate that the photo-activatable technique is also compatible with fluorescence microscopy of focal adhesions (**Figure 4**c).

The flexible and miniaturized design of the migration space allowed us to perform unique geometry-dependent migration studies in a simple way. In the following we describe three examples: (i) migration over constrained geometries, (ii) migration of specific cell areas (front, middle, rear) on lines of widths of subcellular dimensions, and (iii) migration over non-adhesive gaps of increasing sizes. Figure 4a,b and Movies 5 to 7 show migration of HUVECs on lines of 15, 45, and 150 μm width which were scanned perpendicularly to a cell strip pattern. Migration was followed by time lapse microscopy. On line patterns with 15 μm width (Movie 5), single cell migration events were observed. No migration was observed on narrower lines. On lines of 45 and 150 μm width (Movies 6 and 7), the cell front protruded into the migration path (collective migration), but it was not able to move forward in the migration space. In addition, single cells did not escape from the monolayer. After 14 h, the migrating cells at the front rolled back into the monolayer within 2 h (Movie 7). In migratory spaces of 800 μm width (Movie 4), collective migration and complete gap closure was observed. Similar assays were successfully performed with HeLa and HT1080 cell lines (data not shown). These results demonstrate that single or collective migration from the cell layer is strongly influenced by the size of the space available
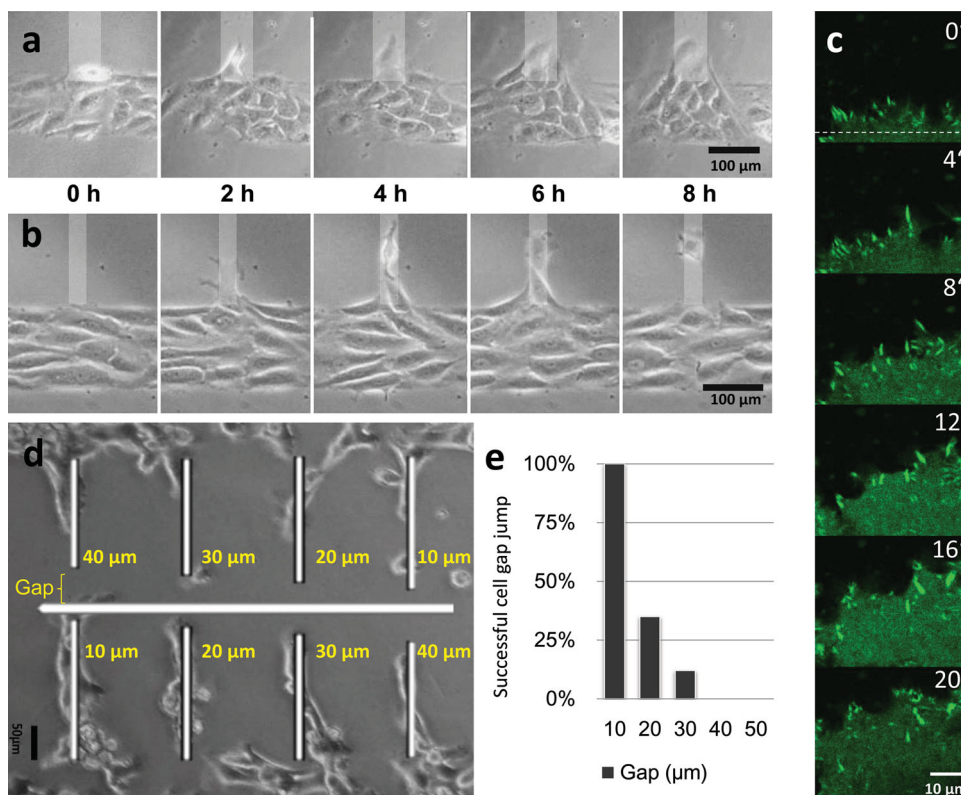
Figure 4. Migration experiments with unconventional designs and geometries. a,b) Migration of HUVECs over a) 15 and b) 45 μm side lines of uncaged cyclo[RGD(DMNPB)fK]. Pictures (from left to right) correspond to every 2 h after side line irradiation. Scale bar 100 μm. Movies 5 to 7 (see the Supporting Information) show the complete experiment. c) Time lapse fluorescence confocal microscopy images of a migrating cell from a stripe pattern. The formation of focal adhesions was observed on the forward progression of the cell. White dotted line shows the edge of the stripe. Scale bar corresponds to 10 μm. Movie 10 shows the complete progression during 20 min. d) "Jump the gap" assay performed on a caged RGD-modified NEXTERION slide with HeLa cells. 15 μm side lines (in white) were irradiated towards a midline (white) leaving a central gap of increasing length from 10 to 50 μm. Single cell migration was observed on the sideline until cells approached the gap. Only gaps smaller than 30 μm were crossed by the cells to the midline. Movie 9 also shows this experiment. e) Percentage of cells that was able to jump to the midline on d) for the different gap lengths.

for migration, in agreement with recently reported results.[27] In addition, these experiments demonstrate the possibility of our method to trigger single cell migration events by opening narrow migration spaces.

Further narrowing of the scanned migration pathways to subcellular dimensions would allow evaluation of migratory responses of different cell areas (front, middle or rear) as shown in Movie 8 in the Supporting Information using HeLa cells. These findings require further investigation and they could shed light on migration selectivity processes starting from the edge of a polarized cell. In a different example, we tested the ability of cells to overcome non-adhesive gaps of increasing length during migration. Lines of 15 μm width were scanned perpendicularly to a cell strip pattern. The strips approached a central line (also irradiated) but did not come into direct contact with it (Figure 4d). Instead, a gap with increasing length (10 to 50 μm) to the central line was generated. Single cells (HeLa) migrated out of the monolayer into the 15 μm lines and passed gaps shorter than 30 μm by stretching its front part to establish an adhesive front and then pulling the cell body over the non-adhesive gap (Figure 4d,e; Movie 9). Longer gaps were not crossed and cells either remained at the end of the line or moved back along the approach path.

3. Conclusions

The photo-activatable cell migration assays allow direct control over molecular interactions involved in cell migration and, specifically, allows dynamic integrin-mediated adhesion and migration studies. Highly miniaturized migration studies, with minimal cell and reagent consumption and a high degree of multiplexing can be performed. It enables nonconventional migration studies in user-defined geometries, including curved and complex designs. It allows free regulation and dynamic variation of the time and space for migration. Complete manipulation under the microscope and it is compatible with high resolution fluorescence microscopy. In addition, it overcomes important limitations of the scratch assay for conventional migration studies (**Table 1**), such as the mechanical damage of cells, the inhomogeneity of the scratched space, and the variation in the adhesive factors necessary for migration. Consequently, this photo-activatable assay reduces variability and improves reproducibility of the migration experiments.

The photo-activatable cell migration assays will allow detailed studies on the correlation between dynamics of integrin-mediated adhesions and single and collective migration modes that could be extended to 3D using multiphoton exposure.

**ADVANCED
FUNCTIONAL
MATERIALS**

www.afm-journal.de

Materials Views

www.MaterialsViews.com

FULL PAPER

Table 1. Compared properties of the photoactivatable cell migration assay (PACMA) and the scratch assay.

Features	Scratch assay	PACMA
Cell type suitable for analysis	Adherent cells	Adherent cells
Sample pool for analysis	Population or individual cell	Population and single cell promoted migration
Ability to track individual cells	Difficult	Yes
Gradients	No	Yes
Sample size in one assay	One condition per culture plate	Substrate availability ruled by light
Complexity of equipment set up	Easy	3 steps substrate preparation, easy to set up
Incubation time before the assay	1–2 days	4 h to 12 h
Time of the assay	Cell types-dependent (8–24 h)	Cell types-dependent (8–24 h)
Data collection and analisys	Time-Lapse microscopy after the scratch. Image procesing	Time-Lapse micros-copy monitoring over the whole process. Image procesing
Cost of equipment	No extra cost than routine tissue culture, inexpensive	UV-led or laser and NHS reactive slides commertially available or by SAMS preparation
Cell damage	Cell stress by stretching, cell death and remaining cell debris after the scratch	No damage

These are relevant issues for tissue regeneration, basic embryogenesis, cancer research and other fields related to cellular dynamics and development.

4. Experimental Section

Cyclo[RGD(DMNPB)fK] Functionalized Commercially Available NEXTERION Slides: Cyclo[RGD(DMNPB)fK] was synthesized as reported elsewhere.[10,17] N-hydroxysuccinimide (NHS) functionalized NEXTERION Slide H (Schott, Material code: 1070936) were equilibrated in phosphate buffer and incubated with a bovine serum albumin (BSA, Sigma A2153) and cyclo[RGD(DMNPB)fK] solution in PBS for 1 h in the dark. The addition of BSA was necessary in order to avoid non-specific attachment of cells to the cyclo[RGD(DMNPB)fK] modified surfaces. The concentration and ratio of BSA and cyclo[RGD(DMNPB)fK] in the mixture was optimized for each cell type: cyclo[RGD(DMNPB)fK] (0.01 mg/mL) and BSA (1 mg/mL) for HUVEC and cyclo[RGD(DMNPB)fK] (0.01 mg/mL) and BSA (2.5 mg/mL) for HT1080 and HeLa cells. Substrates were washed with distilled water and used immediately for cell experiments.

Cyclo[RGD(DMNPB)fK] Functionalized SAMs: Glass slides (12 mm diameter) were cleaned by soaking in Piranha solution (H_2SO_4 (98%)/ H_2O_2 (30%) 5/1) overnight, rinsing with Milli-Q water, absolute ethanol and dried with a N_2 stream. Coating with gold was performed by sequential deposition of chromium (20 Å) and gold (200 Å) films

onto clean glass slides of round shape (diameter 12 mm) via a thermal evaporator (Edward FL 400, 5×10^{-6} mbar, 2 Å/s). Gold-coated substrates were incubated overnight in a mixed thiol (1.0 mM) solution of 99% $HS(CH_2)_{11}(OCH_2CH_2)_3OH$ and 1% $HS(CH_2)_{11}(OCH_2CH_2)_6OCH_2COOH$ thiols (ProChimia TH 001-m11.n3-0,2 and TH 003-m11.n6-0,1) in absolute ethanol. The substrates were rinsed with ethanol and Milli-Q water and then incubated in an aqueous solution of 0.2 M EDC (N-(3-dimethylaminopropyl)-N′-ethylcarbodiimide hydrochloride), 0.1 M NHS (N-hydroxysuccinimide), 2-(N-morpho)-ethanesulfonic acid (0.1 M) and NaCl (0.5 M). After 15 min. the solution was removed and the substrates were washed with deionized water and incubated in a solution of cyclo[RGD(DMNPB)fK] (0.5 mg/mL). The substrates were rinsed with PBS and dried with an N_2 stream. The slides were placed in a 24-well plate for handling and used immediately after modification for cell experiments.

Cell Culture Conditions: HUVECs were isolated and cultured in M199 basal medium (Sigma, M4530) supplemented with L-glutamine (2 mM), penicillin (1000 U/L), streptomycin (100 mg/L, Sigma), ECGS supplement (Sigma, E-2759), sodium heparin (Sigma, H-3393) and 20% fetal calf serum (FCS) as previously described [8]. HUVEC were used between passages 2 to 6. HT1080 and HeLa cells were cultured in DMEM medium (Invitrogen) supplemented with 10% fetal bovine serum (FBS), 1% L-glutamine from Invitrogen at 37 °C in 5% CO2.

Cyclo[RGDfK] Surface Patterns by Laser Scanning: A silicon gasket was adhered to the dry cyclo[RGD(DMNPB)fK]-modified NEXTERION substrate in order to compartimentalize the surface and allow replicas and different treatment over the same slide. The substrates loaded with cells were placed on a sealed microscope stage incubator at 37 °C and 5% CO_2 environment (Ibidi, Heating & Incubation system). The set-up was also equipped with a 403 nm laser that allowed automated writing of micrometric patterns with adjustable light intensity (see reference for a detailed description of the microscope setup).[28] Cell dynamics was followed in situ by phase contrast microscopy. Alternatively, the substrates were placed on the confocal microscope for imaging after exposure.

Cyclo[RGDfK] Surface Patterns by Masked Exposure: In order to save microscope time during monolayer formation, the first irradiation step to generate RGD patterns was also performed using a LED lamp and a mask. A quartz substrate containing a chrome masks with stripes or circles (ML&C, Jena) was placed on the RGD modified substrate before irradiation with a 365 nm LED source (NT65-940, Edmund Optics, Irradiance ≈ 4.5 mW cm^{-2}) for 4 min. The substrate was washed with distilled water and used immediately for the cell experiments.

Cell Seeding and Preparation for Time-Lapse Microscopy: Patterned RGD modified SAMs in a 24-well plate were incubated overnight with 500 μL of a 5×10^4 cells/mL suspension of HUVECs or 1.5×10^5 cells/mL suspension of HT1080 cells. The substrates were rinsed with PBS and fresh medium to obtain neat patterns and remove cell debris. The patterns were imaged by phase contrast microscopy and confocal microscopy. Comparable conditions were used for the NEXTERION slides.

Photo-Activatable Cell Migration Assay as Followed by Time Lapse Microscopy: Patterned RGD substrates containing with 600 μm RGD functionalized strips separated by 400 μm gaps were incubated with HUVECs overnight, washed and placed in the custom-built setup stage. The second irradiation step for initiating migration was performed either with a 403 nm scanning laser or by direct exposure to a 365 nm LED lamp placed on the top of the substrate using the microscope light path. Microscopic images were taken every minute with an Oscar digital camera (Allied Vision Technologies, Stadtroda, Germany) mounted on a Leica DM-IRB inverted microscope (Wetzlar, Germany) with a 10× or 5× objective (Leica, NA 0.4).

Scratch Test: HUVECs were seeded in 35 mm diameter culture petri dishes and cultured until confluence. The cells were then scraped with a 200 μL micropipette tip, denuding a strip of the monolayer. The cells were time-lapse–monitored every minute for 24 h in the set-up described above. Alternatively (data in Figure 3d), the same test was performed on SAMs modified with commercially available cyclo[RGDfK] (Peptides International, USA).

www.MaterialsViews.com

ADVANCED
FUNCTIONAL
MATERIALS
www.afm-journal.de

FULL PAPER

Fluorescent Actin Staining: Cells cultured on glass coverslips were permeabilized with 0.5% Triton X-100 and fixed with 4% paraformaldehyde (PFA) in PBS during 5 min. The coverslips were incubated with TRITC-conjugated phalloidin (Millipore) during 10 min to stain actin cytoskeleton in red.

Microscopy and Quantification of Imaged Data: Time-lapse movies recorded during migration studies were segmented as follows. Pictures were obtained every 15 min for single cell monitoring or every 2 h for wound healing. The uncovered wound area was measured and quantified at different intervals for 24 h using ImageJ software (NIH). The migration rate was calculated as the cell covered area from the wound vs. time.

Live/Dead Assay: After the scratch cell were washed with PBS and Propidium iodide (e.g., Cat # 537059, Calbiochem, San Diego, CA) was added. 15 min after pictures were taken using an epi-fluorescent microscope irradiating at 535 nm. Only death cells appeared red. Stained nucleuses were obtained after fixation with MeOH and mounted using DAPI Fluoromount-G (SouthernBiotech Cat # 0100-01).

Supporting Information

Supporting Information is available from the Wiley Online Library or from the author.

[1] A. J. Ridley, M. A. Schwartz, K. Burridge, R. A. Firtel, M. H. Ginsberg, G. Borisy, J. T. Parsons, A. R. Horwitz, *Science* **2003**, *302*, 1704.
[2] P. Rorth, *Dev. Cell* **2011**, *20*, 9.
[3] P. Friedl, D. Gilmour, *Nat. Rev. Mol. Cell Biol.* **2009**, *10*, 445.
[4] A. Huttenlocher, A. R. Horwitz, *Cold Spring Harb. Perspect. Biol.* **2011**, *3*, 005074.
[5] C. G. Rolli, H. Nakayama, K. Yamaguchi, J. P. Spatz, R. Kemkemer, J. Nakanishi, *Biomaterials* **2012**, *33*, 2409.
[6] J. E. Frith, R. J. Mills, J. J. Cooper-White, *J. Cell Sci.* **2012**, *125*, 317.
[7] A. Huttenlocher, M. H. Ginsberg, A. F. Horwitz, *J. Cell Biol.* **1996**, *134*, 1551.
[8] M. R. Ng, A. Besser, G. Danuser, J. S. Brugge, *J. Cell Biol.* **2012**, *199*, 545.
[9] P. Friedl, K. Wolf, *J. Cell Biol.* **2010**, *188*, 11.
[10] S. Petersen, J. M. Alonso, A. Specht, P. Duodu, M. Goeldner, A. Del Campo, *Angew. Chem. Int. Ed.* **2008**, *47*, 3192.
[11] S. Raghavan, R. A. Desai, Y. Kwon, M. Mrksich, C. S. Chen, *Langmuir* **2010**, *26*, 17733.
[12] M. N. Yousaf, B. T. Houseman, M. Mrksich, *Angew. Chem. Int. Ed.* **2001**, *40*, 1093.
[13] E. W. L. Chan, S. Park, M. N. Yousaf, *Angew. Chem. Int. Ed.* **2008**, *47*, 6267.
[14] Y. Ohmuro-Matsuyama, Y. Tatsu, *Angew. Chem. Int. Ed.* **2008**, *47*, 7527.
[15] D. B. Liu, Y. Y. Xie, H. W. Shao, X. Y. Jiang, *Angew. Chem. Int. Ed.* **2009**, *48*, 4406.
[16] T. Vignaud, R. Galland, Q. Z. Tseng, L. Blanchoin, J. Colombelli, M. Thery, *J. Cell Sci.* **2012**, *125*, 2134.
[17] M. Wirkner, J. M. Alonso, V. Maus, M. Salierno, T. T. Lee, A. J. Garcia, A. del Campo, *Adv. Mater.* **2011**, *23*, 3907.
[18] M. Wirkner, S. Weis, V. San Miguel, M. Alvarez, R. A. Gropeanu, M. Salierno, A. Sartoris, R. E. Unger, C. J. Kirkpatrick, A. del Campo, *ChemBioChem* **2011**, *12*, 2623.
[19] J. P. Xiong, T. Stehle, R. Zhang, A. Joachimiak, M. Frech, S. L. Goodman, M. A. Arnaout, *Science* **2002**, *296*, 151.
[20] M. Murrell, R. Kamm, P. Matsudaira, *PloS One* **2011**, *6*, e24283.
[21] C. C. Liang, A. Y. Park, J. L. Guan, *Nat. Protoc.* **2007**, *2*, 329.
[22] http://www.ibidi.com/products/disposables/E_802XX_CI_family.html (accessed June, 2013).
[23] http://www.cellbiolabs.com/wound-healing-assays?gclid=CI_V3Z3ljbECFUIN4AodTwq3Cw (accessed January, 2013).
[24] C. R. Keese, J. Wegener, S. R. Walker, I. Giaever, *Proc. Natl. Acad. Sci. USA* **2004**, *101*, 1554.
[25] B. Guillotin, F. Guillemot, *Trends Biotechnol.* **2011**, *29*, 183.
[26] M. Poujade, E. Grasland-Mongrain, A. Hertzog, J. Jouanneau, P. Chavrier, B. Ladoux, P. Buguin, P. Silberzan, *Proc. Natl. Acad. Sci. USA* **2007**, *104*, 15988.
[27] S. R. Vedula, M. C. Leong, T. L. Lai, P. Hersen, A. J. Kabla, C. T. Lim, B. Ladoux, *Proc. Natl. Acad. Sci. USA* **2012**, *109*, 12974.
[28] M. Alvarez, J. M. Alonso, O. Filevich, M. Bhagawati, R. Etchenique, J. Piehler, A. del Campo, *Langmuir* **2011**, *27*, 2789.